JPE 16-5-26

http://dx.doi.org/10.6113/JPE.2016.16.5.1869
ISSN(Print): 1598-2092 / ISSN(Online): 2093-4718

A Voltage Regulation System for Independent Load Operation of Stand Alone Self-Excited Induction Generators

Selami Kesler† and Tayyip L. Doser*

†,*Department of Electrical and Electronics Engineering, Pamukkale University, Denizli, Turkey

Abstract

In recent years, some converter structures and analyzing methods for the voltage regulation of stand-alone self-excited induction generators (SEIGs) have been introduced. However, all of them are concerned with the three-phase voltage control of three-phase SEIGs or the single-phase voltage control of single-phase SEIGs for the operation of these machines under balanced load conditions. In this paper, each phase voltage is controlled separately through separated converters, which consist of a full-bridge diode rectifier and one-IGBT. For this purpose, the principle of the electronic load controllers supported by fuzzy logic is employed in the two-different proposed converter structures. While changing single phase consumer loads that are independent from each other, the output voltages of the generator are controlled independently by three-number of separated electronic load controllers (SELCs) in two different mode operations. The aim is to obtain a rated power from the SEIG via the switching of the dump loads to be the complement of consumer load variations. The transient and steady state behaviors of the whole system are investigated by simulation studies from the point of getting the design parameters, and experiments are carried out for validation of the results. The results illustrate that the proposed SELC system is capable of coping with independent consumer load variations to keep output voltage at a desired value for each phase. It is also available for unbalanced consumer load conditions. In addition, it is concluded that the proposed converter without a filter capacitor has less harmonics on the currents.

Key words: Fuzzy logic, Independent load operation, Separated electronic load controller, Stand-alone induction generators, Voltage regulation

I. INTRODUCTION

Many alternative energy sources to meet the increasing energy demands such as hydro, wind, solar, geothermal, biomass, etc., have been becoming more and more important because of the rapid depletion of fossil fuels. For power generation from these energy sources, synchronous generators have been used conventionally. On the other hand, due to some of the outstanding features of induction generators, such as brushless and rugged construction, self-protection against over currents, low cost maintenance and ability to generate power under varying drive conditions, they have been widely used to generate electricity from these sources [1]-[3]. For this purpose, induction generators have been operated in different modes: stand-alone operation mode (off-grid), operation mode in parallel with synchronous generators and on-grid mode operation [4]. In the first and second half parts of the 20th century, the modelling and analysis of induction machines were manifested in literature in terms of self-exciting requirements and stand-alone or grid-connected operation conditions [5], [6]. In particular, the capacitor requirements for self-excitation and maintaining reactive power in the off-grid mode and its effects on machine performance of the connection nodes of the capacitors, i.e. long or short shunt, were investigated and sufficient values for the capacitors together with connection nodes for achieving better performance, realizing more voltage compensation and providing maximum power to the loads were brought into the researchers' view [7]-[10].

Manuscript received Sep. 16, 2015; accepted Jun. 9, 2016
Recommended for publication by Associate Editor Dong-Myung Lee.
†Corresponding Author: skesler@pau.edu.tr
Tel: +90-258-296-3034, Fax: +90-258-296-3262, Pamukkale Univ.
*Department of Electrical and Electronics Engineering, Pamukkale University, Turkey

In order to achieve control of the frequency and voltage of wind-driven wound-rotor induction generators, solid-state converters have been used in both the rotor and stator side. However, the harmonic effects of the converters and their costs in low power applications and the maintenance of the rings are drawbacks to utilizing this type induction generators [11], [13]. In contrast, the squirrel-cage or variable speed-cage types of induction generators are available for low power and stand-alone operations [14]. However, the solid-state converters being used in either the stator side or both sides are suitable for implementing intelligent techniques to controlling the terminal voltage and frequency with an improved power quality by advanced microprocessors, which are genetic algorithms or fuzzy based supervisors and direct voltage controllers [15]-[18]. Despite the high computational burden, the control performance of these methods are quite high.

One of the interesting voltage control methods for induction generators is to employ a three-phase magnetic flux controlled type variable reactor [19]. However, the drawback of the method is that an external power source for voltage control is needed. The most widely used voltage control method for SEIGs is to adjust the terminal impedance by using dumping loads. The fundamentals of this method were first explained by Bonert et al. [20], [21], in the 1990s. Afterwards, this method has been called "electronic load control- ELC". However, in recent years, many important studies on ELC for SEIGs for the investigation of both the static and dynamic load operation principles were manifested by Singh, Murty and Gupta [22], [24]. In addition, the transient and steady state behaviors of a system controlled by ELC for balanced load operations were successfully explained.

ELC includes a system to keep the output power of the generator constant at every change in a consumer load. For this purpose, three or single-phase dump loads on the terminal are used as a complementary of the consumer loads connected to the SEIG so that the output power is at its maximum at every step-changes in consumer loads. In addition, ELC is also available for wind-driven SEIGs without changing the pitch angle of the wind turbine blades [25]. PI or intelligent based methods have been used for both single-phase and three-phase balanced consumer loads to improve the efficiency of the ELCs [26]-[31]. Using multi-pulse ELC to control the terminal voltage of SEIGs has been performed only for balanced three-phase consumer loads [32]. In addition, for large load changings in single-phase consumer loads, a dynamic controller with single-phase inverters was introduced [33], [34]. However, unbalanced three-phase and independent single-phase load variations for squirrel-cage stand-alone induction generators have yet to been sufficiently analyzed. However, the unbalanced operation of stand-alone doubly fed induction generators used in rotor and stator side converters were analyzed by Pena et al. in [35]. On the other hand, in case of the existence of independent loads of consumers, unbalanced operations and the necessity of separated ELCs are also inevitable in SEIGs.

Therefore, in this study the independent-separated ELCs supported by fuzzy logic controllers, which are available for both the balanced and independent single-phase load conditions of consumers, are designed and implemented. The fuzzy logic control method is preferred to regulate the terminal voltage because this expert control system does not require a dynamic model of the system and it is insensitive to parameter changes of the system. However, this study does not focus on the control method.

Since the mechanical power input does not vary on a large scale and the output power of the generator must be kept constant for all consumer load conditions, the excitation capacitors connected to the terminal of a SEIG are used at a fixed value to provide a nominal frequency and voltage at full load. The differences from the existing literature and the novelty of the study are, first, to control the output voltage per phase independently by separated ELCs, which is available for independent single phase consumer load variations, and to present an analysis of the proposed two-different converter structures with and without a filter capacitor at the end of the diode rectifiers, by supporting a fuzzy logic controller, which is insensitive to the parameters of the system architectures. On other hand, the behavior of the proposed converter with a capacitor is newly presented in this paper. Details of the purposed systems are introduced in the following sections.

II. DESCRIPTION OF THE PROPOSED SYSTEM

The principle of the system is that the surplus power of the generator is dumped in the resistances through the (separated electronic load controllers) SELCs, where the consumers cannot draw full power from the generator. Thanks to this dumping process, the amplitude of the output voltages of the SEIG are kept nearly constant in defined limits at any consumer load variation. On the other hand, if the consumer loads draw full power from the SEIG, the dumping loads are not switched to the ON state, i.e. the dump load currents are held at nearly the zero level. Nevertheless, in the case of the unbalanced operation of the SEIG, the phase voltages can increase or decrease differently from each other. For this reason, a SELC for each phase is proposed in this study. The principle schema is shown in Fig. 1. The control system uses a capacitor bank with a fixed value, which is used to provide reactive power for self-excitation and to keep the frequency constant for full loading, three-phase separated dump load systems, which are switched by the fuzzy logic control software embedded in the microprocessor, and three

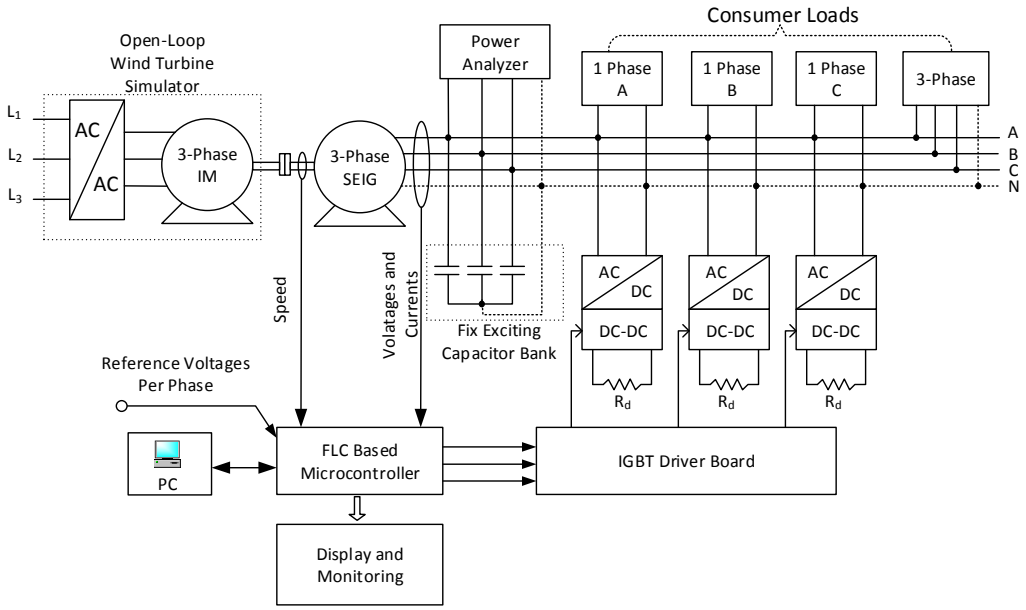

Fig. 1. Principle schema of for the voltage regulation of the SEIG with SELC.

separated single-phase uncontrolled rectifiers with one IGBT per phase.

In this study, instead of using bidirectional switches, AC to DC single-phase rectifiers are used independently from each other in each phase, and DC to DC choppers are connected across the output of these rectifiers. Thus, the dumping loads are switched by only one IGBT to regulate the output voltage of the SEIG for each phase. This reduces the costs of the converters and their driving boards. For the simulation and experimental studies, the SEIG is driven by an induction motor through an industrial type constant V/f-based variable speed drive as a prime mover in place of a wind turbine model. The microprocessor used in the controller interface is embedded with fuzzy logic algorithms to assess the errors between the generated and reference voltages accepted by the users.

Three PWM signals with different variable duties for voltage regulation in each phase are produced and applied to the gates of the IGBTs through the driver board. Thus, the rated power of the generator provides full power to the consumer loads along with the dump loads switched as a complement of the consumers under every load variation.

A. Dynamic Model of the SEIG

The stator and rotor voltage equations of the SEIG in the abc-real axes can be expressed in Equs. (1) and (2).

$$v_{abcs} = r_s i_{abcs} + \frac{d\psi_{abcs}}{dt} \tag{1}$$

$$0 = r_r i_{abcr} + \frac{d\psi_{abcr}}{dt} \tag{2}$$

The difficulty in the solution of these equations is because of the dependency on the time and rotor position of the inductances. As a result, different axes transformations are involved to simplify these equations. By the phase transformation, the inductances become independent from the time and rotor position. Therefore, the reference frame axes are fixed on the stator and it is called the stationary axes. At the end of the d-q transformation, equations (1) and (2) are written in the stationary axes frame for balanced operation as follows [5].

$$\frac{d\psi_{ds}}{dt} = v_{ds} - r_s i_{ds} \tag{3}$$

$$\frac{d\psi_{qs}}{dt} = v_{qs} - r_s i_{qs} \tag{4}$$

$$\frac{d\psi_{dr}}{dt} = -r_r i_{dr} - \omega_r \psi_{qr} \tag{5}$$

$$\frac{d\psi_{qr}}{dt} = -r_r i_{qr} + \omega_r \psi_{dr} \tag{6}$$

Where, s marks the stator variables, r marks the rotor variables, ψ marks the flux linkages, ω_r is the rotor electrical angular frequency, and r_r and r_s are the rotor and stator copper resistances, respectively.

Since the magnetizing inductance depends on stator flux linkage, it can be defined in terms of using the space vector description as follow:

$$L_m = f(|\Psi_s|) \tag{7}$$

Although the magnetizing inductance has a nonlinear curve, by the linear approximation in each solution step for the equations, the d-q component of the magnetizing flux linkage can be addressed by multiplying the instantaneous magnetizing inductance with the related components of the stator currents.

$$\psi_{dm} = L_m i_{dm} \tag{8}$$

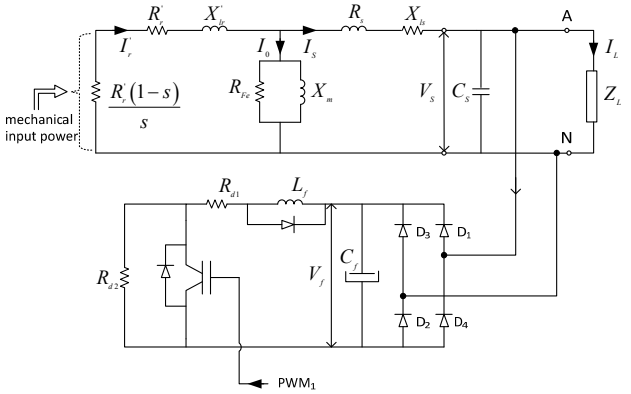

Fig. 2. Equivalent circuit per phase for the SEIG with SELC.

$$\psi_{qm} = L_m i_{qm} \tag{9}$$

Thus, the d-q component of the stator flux linkage can be written as in (10) and (11) in terms of the stator leakage inductance and magnetizing component of the flux linkage.

$$\psi_{ds} = -L_{ls} i_{ds} + \psi_{dm} \tag{10}$$

$$\psi_{qs} = -L_{ls} i_{qs} + \psi_{dm} \tag{11}$$

By this way, rotor flux linkages in the d-q frame axes are expressed as follows:

$$\psi_{qr} = L_{lr} i_{qr} + \psi_{dm} \tag{12}$$

$$\psi_{dr} = L_{lr} i_{dr} + \psi_{dm} \tag{13}$$

The developed torque in the shaft by the generator can be expressed in terms of the d-q currents and flux components as follows:

$$T_{gen} = \frac{3}{2} P_0 (\psi_{ds} i_{qs} - \psi_{qs} i_{ds}) \tag{14}$$

On the other side, the torque induced by the prime mover can be given in Equ. (15).

$$T_{mov} = T_{gen} + \beta \omega_m + j \frac{d\omega_m}{dt} \tag{15}$$

Where, β is the total friction coefficient of the mechanical system, ω_m is mechanical speed of the prime mover, j is the effective inertia of the system, and P_0 is the number of pole pairs.

B. Exciting Capacitor, Consumer and Dump Loads

An equivalent circuit diagram is shown in Fig. 2. The required capacitor for self-excitation of the induction generator is defined to provide the necessary reactive power to the system and to keep the frequency nearly constant at the terminal of the SEIG under the full load condition. In the d-q reference frame, the current equation of the self-exciting capacitor is expressed by the related voltage component as follows:

$$\frac{dv_{ds}}{dt} = \frac{1}{C_s} i_{dc} \tag{16}$$

$$\frac{dv_{qs}}{dt} = \frac{1}{C_s} i_{qc} \tag{17}$$

At the same time, since the capacitor bank is connected in parallel with the consumer load and dumped load by the SELC, the current equations at the node can be written as in (18) and (19) in terms of their related d-q components.

$$i_{dc} = i_{ds} - i_{dL} - i_{dD} \tag{18}$$

$$i_{qc} = i_{qs} - i_{qL} - i_{qD} \tag{19}$$

The derivative expressions of the consumer load currents can be calculated in terms of the load resistance and inductance as follows.

$$\frac{di_{dL}}{dt} = \frac{1}{L_L}(v_{ds} - R_L i_{dL}) \tag{20}$$

$$\frac{di_{qL}}{dt} = \frac{1}{L_L}(v_{qs} - R_L i_{qL}) \tag{21}$$

The dumping load current is obtained depending on the output voltage of the rectifier, the dump load resistance and the filter inductance with the related d-q components.

$$\frac{di_{dD}}{dt} = \frac{1}{L_f}\left[V_{df} - (R_{d1} + S.R_{d2}) i_{dD}\right] \tag{22}$$

$$\frac{di_{qD}}{dt} = \frac{1}{L_f}\left[V_{qf} - (R_{d1} + S.R_{d2}) i_{qD}\right] \tag{23}$$

Where, S describes the switching state of the IGBT operating as a chopper in the SELC. When the switch is ON, S takes the value of 1. In other cases, S is equal to zero. On the other hand, the used inductor in serial with the pre-dump resistance (R_{d1}) is too small for only the turn-on snubber of the switch.

In practice, the consumer loads may be single-phase and may each change differently. In addition, the consumer load impedances consisting of resistance and inductance have different values. Furthermore, they can be made up of dynamic and static loads.

For converting the d-q components of the currents and voltages into the abc-axes, the matrix equation below can be used.

$$\begin{bmatrix} i_a \\ i_b \\ i_c \end{bmatrix} = \begin{bmatrix} 1 & 0 \\ -\frac{1}{2} & \frac{\sqrt{3}}{2} \\ -\frac{1}{2} & \frac{\sqrt{3}}{2} \end{bmatrix} \begin{bmatrix} i_{ds} \\ i_{qs} \end{bmatrix} \tag{24}$$

Afterwards, the voltages and currents of consumers are calculated by the matrix equation related to the phase currents as follow:

$$\begin{bmatrix} v_a \\ v_b \\ v_c \end{bmatrix} = \begin{bmatrix} R_a + L_a p & 0 & 0 \\ 0 & R_b + L_b p & 0 \\ 0 & 0 & R_c + L_c p \end{bmatrix} \begin{bmatrix} i_a \\ i_b \\ i_c \end{bmatrix} \tag{25}$$

Where, P is the time derivative, and $R_{a,b,c}$ and $L_{a,b,c}$ are the resistances and inductances of the respective phases. On the other hand, in case of unbalanced three-phase operation, the SEIG model is rewritten in terms of symmetrical components for obtaining a converted system model in which the system behaves like it is balanced.

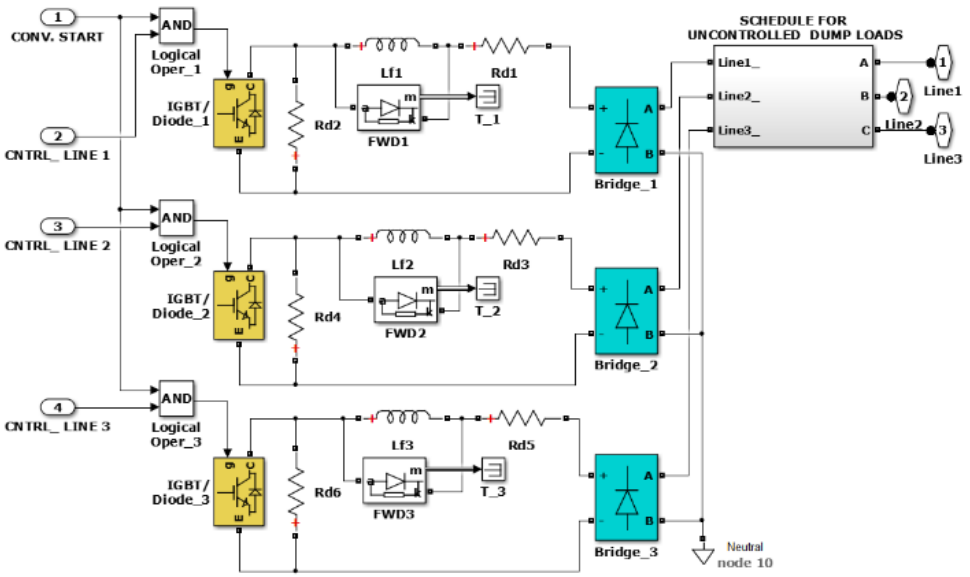

Fig. 3. Internal structure of the SELCs for each phase.

C. Control Strategy of SELC

For every load variation, the output power of the generator is kept constant to regulate the terminal voltage across the consumer load. At the same time, the input power of the SEIG is nearly constant. However, for using a wind turbine as the prime mover, the input power changes depending on the turbine and instantaneous wind parameters. In order to represent a wind turbine, an induction motor with a variable speed drive is used. The more the SEIG is loaded, the harder the output voltage falls and the more the shaft speed of the generator decreases. Therefore, depending on this behavior, the output frequency decreases. A capacitor bank defined at a fixed value is connected across the terminal to maintain a constant frequency and to recover a modicum of the output voltage. The generated power from the SEIG is kept at its maximum or at its rated value in all cases. When the consumer power increases, the power controlled by the SELC decreases. The opposite is also true. The loading of the consumers and the ELCs are the complements of each other. The internal structure of the SELC circuits is shown in Fig. 3. Regardless of the power losses, the generator provides the needed power for consumers and ELC to keep the terminal voltage constant. The equation of the complementary power is given in (26), including loses.

$$Gen.Power(P_{gen}) = Dump\,Load(P_D) + Cons.Load(P_L) + Loses(P_{los}) \quad (26)$$

In Fig. 3, for both single phase independent consumer loads and balanced three-phase consumer loads, the terminal voltages of the SEIG are measured step-by-step. They are then compared with the users or grid references to produce the error together with the change in the error signals for the separated FLC. These signals are evaluated to produce

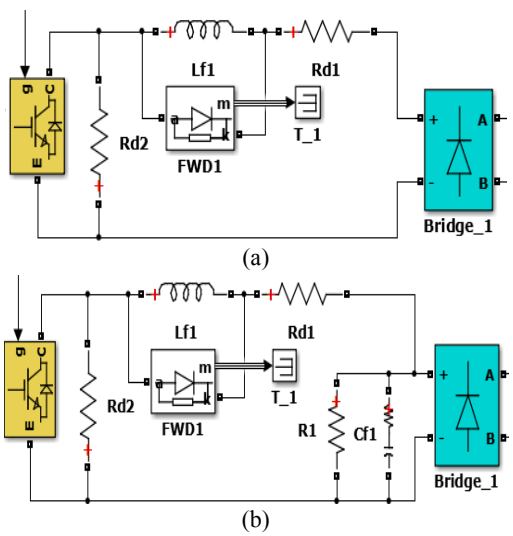

Fig. 4. Two-different converter structures, (a) without filter capacitor (b) with capacitor.

three-independent PWM signals with variable duties. They are then applied to the gates of the IGBTs, which act as a dc chopper. In the chopper circuits, each of the IGBT switches a load of 750 Ω (R_{d2}) in series with 75 Ω (R_{d1}) for controlling an output power of approximately 2000-Watt. A permanent load of 75 Ω as a pre-dump resistance is connected in series with a snubber inductance coupled with a fast recovery diode, as detailed in Fig. 4 (a). In the other structure of the converter, a filter capacitor is used at the end of the bridge rectifier, as detailed in Fig. 4 (b). Simulations and experimental implementations present investigations of both converters.

In the chopping mode without a filter capacitor at the end of the diode bridges, the average value of the dump current in one switching period changes between two levels, as shown in Fig. 5. When the switch turns ON, the R_{d2} dump resistance

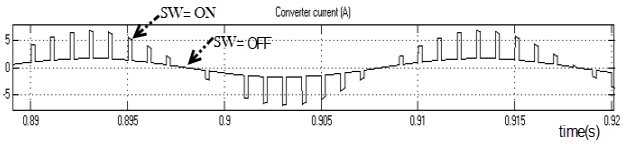

Fig. 5. Converter current for 1 kHz switching frequency in chopping mode without capacitor (R_{d1} =50 Ω, R_{d2} =100 Ω, L_f =1μH).

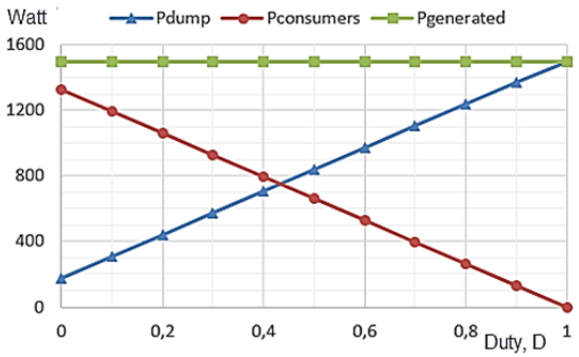

Fig. 6. Dump, consumers and generated power from the SEIG versus duty ratio of SELC.

is short-circuited, and the converter current flows through the pre-dump resistance (R_{d1}), the snubber inductance and the IGBT switch. In the other case, when the switch turns OFF, all of the dump resistances remain in the current way, as shown in Fig. 4. In addition, the diodes and IGBT switch act as a bidirectional switch or a back-to-back reverse IGBT switch module, from the point of view of the front of the converter. Furthermore, in this operation mode a serial inductance with a pre-dump resistance is selected as a turn-on snubber for the main switch. Therefore, it is small enough to ignore inductive effect on the current way.

When the switch is ON during the duty cycle (DT), the expression of the dump load current is written as below.

$$i_{D_{ON}} = \frac{V_s}{R_{d1}} \tag{27}$$

In the rest of the switching period (1-DT), the switch is OFF and the dump load current is obtained as follows:

$$i_{D_{OFF}} = \frac{V_s}{R_{d1} + R_{d2}} \tag{28}$$

Where, T represents the switching period, and D is the duty ratio of the ON time to the period. Thus, the average value of the dump current in one switching cycle is calculated by the following equations:

$$I_D = \frac{1}{T}\left[DT \cdot I_{D_{ON}} + (1-D)T \cdot I_{D_{OFF}}\right] \tag{29}$$

$$I_D = D \cdot I_{D_{ON}} + (1-D) \cdot I_{D_{OFF}} \tag{30}$$

When equations of (27) and (28) are used in (30), the switched admittance of the converter depending only on the dump load resistances and the duty ratio are obtained below.

$$I_D = \frac{V_s}{Z_D} = D\frac{V_s}{R_{d1}} + (1-D)\frac{V_s}{R_{d1} + R_{d2}} \tag{31}$$

In addition, the admittance of the switched dump load in front of the converter is as follows:

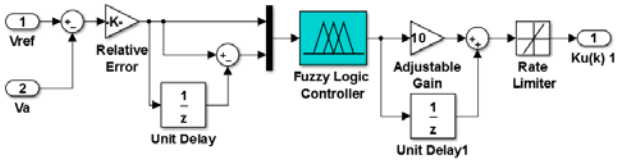

Fig. 7. The principal scheme of the FLC.

$$Y_D = \frac{1}{Z_D} = \frac{R_{d1} + D \cdot R_{d2}}{R_{d1}(R_{d1} + R_{d2})} \tag{32}$$

$$Y_D = k_1 + k_2 D \tag{33}$$

Where, $k_1 = \frac{1}{R_{d1} + R_{d2}}$ *and* $k_2 = \frac{R_{d2}}{R_{d1}} \cdot k_1$, and as can be seen from Eq. (33) the admittance of the switched dump load acts linear versus the duty ratio of the converters. Therefore, the dumped power by the converters (SELCs) per phase is also achieved in a linear fashion as follows, while neglecting the converter loses.

$$P_{gen} \cong P_D + P_L = P_{\max} \tag{34}$$

$$P_D = P_{\min} + D(P_{\max} - P_{\min}) \tag{35}$$

$$P_L = (1-D)\left(P_{\max} - P_{\min}\right) \tag{36}$$

Where, when the main switch is OFF, all of the dump loads absorb power, which is represented by P_{min}. On the other hand, the amount of consumed power by the main consumer loads (P_L) is limited to (P_{max}-P_{min}). In order to keep the terminal voltage and frequency at their initial reference values, the SEIG must generate its maximum power by providing all of the main loads together with the dump loads at any time. For instance, after defining of the maximum main load power, the switched dump resistance (R_{d2}) and pre-dump resistance (R_{d1}) are defined. Thus, the minimum and maximum power absorbed by the dump loads can be calculated. As shown in Fig. 6, since a maximum power of 1500 Watt is obtained from the SEIG, it can be estimated that for R_{d2}=750 Ω, R_{d1}=96 Ω and P_{min}=172 W, approximately. From this reason, the maximum power to be absorbed by the main loads is up to 1328 W, together with the converter loses. If the pre-dump resistance is selected as 75 Ω, the controlled power by the converters closes to 2000 W, and the minimum power absorbed by the SELCs increases to 176 W, which is nearly constant.

III. Design of Fuzzy Logic Controller

The well-known principal model of the fuzzy logic controller (FLC) is shown in Fig. 7. The FLC consists of fuzzification, an inference engine and defuzzification along with a limiter lest the crisp value produced by the engine takes a value that is more than 1, because of the cumulative operation in fuzzy inferences. To adjust the effective value of the terminal voltage, two-signal are passed into the fuzzifier, in which one of these signal is the relative error between the reference and the real terminal voltage, and the other is the

change in the error which results from taking the difference between the previous error value and the error. Holding the terminal voltage at a desired value, the PWM duty is adjusted by the FLC. The intervals of the error and the change in error are defined according to the dynamic behaviors of the SEIG, and the sinusoidal membership functions are selected to fuzzify the error and the change in error. The fuzzy logic rule assignment table is formed after consideration of the control to be done. The output of the defuzzifier is bounded in the interval of [-1, 1] to make the control system operate stably [36], [38].

All of the PWM duties are updated according to the FLC decision for each phase by the application of (37). The crisp value produced by the FLC is used in the scale of a controller coefficient, which is called the controller efficiency constant, δ, and it is added to its previous value to achieve a comparison value for the timer in the microprocessor. The controller efficiency constant is updated from 0.1 to 10 according to the desired controller response.

$$KU_{(k)} = DU_{(k-1)} + \delta DU_{(k)} \tag{37}$$

Considering the variation intervals of the error and the changes in the error in Fig. 7, the sinusoidal membership functions are selected, as shown in Fig. 8. The locations of the fuzzy numbers NN, ZZ and PP in the universe of discourse X are in the order of NN<ZZ<PP from negative *x* to positive *x*. This naming corresponds to Negative, Zero, and Positive, respectively. The number of the membership function is defined for minimization of the control complexity of a low cost microprocessor. Three fuzzy sets are available for this control operation. For symmetrical sinusoids, $d = 2b = 4a$, and the angular cycling frequency of these fuzzy sets can be written as follow:

$$\omega = \frac{\pi}{2a} = \frac{\pi}{b} = \frac{2\pi}{d} \tag{38}$$

For example, at the point of $x = x_1$, where $a \le x \le b$; the membership values of the input of x_1 are calculated by the related sinusoid functions as follows:

$$\begin{aligned} \mu_{NN}(x_1) &= \sin \omega x_1 \\ \mu_{ZZ}(x_1) &= -\cos \omega x_1 \\ \mu_{PP}(x_1) &= 0 \end{aligned} \tag{39}$$

The cycling frequency of the sinusoid functions is defined as $\omega = (\pi / X_{max})$ for each fuzzy function in one cycle. All of the sinusoid membership functions in the control process are employed by taking $X_{max} = 0.005$ for an error corresponding to 0.5%, $X_{max} = 0.002$ for the change in error corresponding to 0.2%, and $X_{max} = 1.0$ for the output of the controller. Thus, the desired base voltage at the terminal is 400-Volt (line to line), and an acceptable voltage drop in the consumer load is 0.5%.

Because of the easy process in a microprocessor, the output membership function is also determined as a singleton model

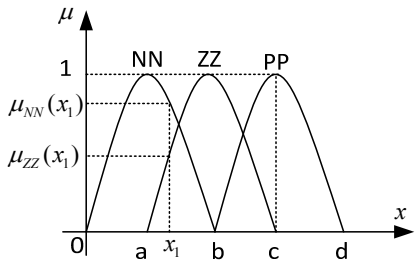

Fig. 8. Fuzzy membership function for inputs of the FLCs.

TABLE I
THE RULE BASE FOR THE FLCS

$e,\ ce$	NN_{ce}	ZZ_{ce}	PP_{ce}
NN_e	PP_{du}	$\frac{PP_{du}}{2}$	$\frac{PP_{du}}{5}$
ZZ_e	$\frac{PP_{du}}{2}$	ZZ_{du}	$\frac{NN_{du}}{2}$
PP_e	$\frac{NN_{du}}{5}$	$\frac{NN_{du}}{2}$	NN_{du}

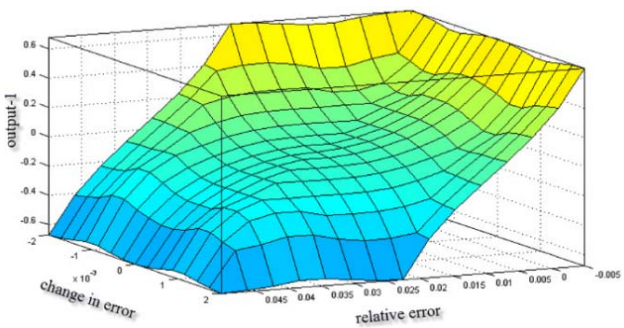

Fig. 9. Decision surfaces of the FLC by MATLAB/Simulink.

of Takagi and Sugeno [39]. The rule assignment table with nine rules shown in Table I is obtained according to the control is realized by experience and used for all membership functions without altering its structure. These rules are included in the algorithm of the solution as follows:

if $e(k)$ *is in set of NN? and?* $e(k)$ *is in set of PP then*

$$\left\{ \begin{array}{l} du(k) = 0; \ // \ du(k) \ is \ in \ \text{set of } ZZ \\ \mu du(k) = min(\mu eN, \mu deP); \end{array} \right\}$$

The output sets of the FLC are scaled by coefficients, such as 2 and 5, as given in Table I. Thus, the control, which is more effective, is provided with a reduced number of rules to achieve softer switching in place of more crisp values at the end of the fuzzy inference.

For the fuzzy inference engine, the Max-min method of Mamdani [40] is preferred. The defuzzification is done by the center of gravity method as given by equation (40). A fuzzy decision surfaces via MATLAB Simulink is shown in Fig. 9.

$$DU(k) = \frac{\sum_{k=1}^{n} du(k) * \mu_{du}(k)}{\sum_{k=1}^{n} \mu_{du}(k)} \tag{40}$$

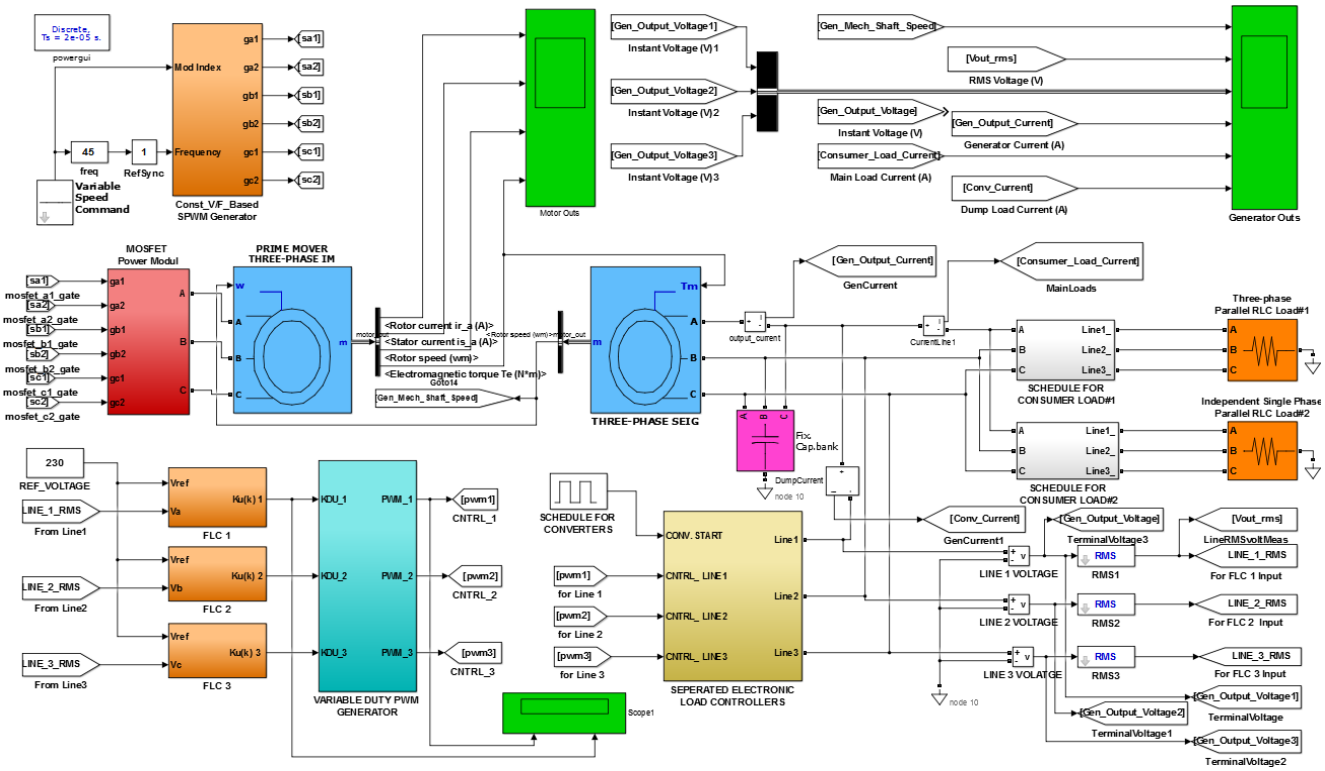

Fig. 10. Matlab/Simulink block diagram of the whole system.

IV. Simulation Models and Results

For simulation studies and for determining the design parameters of the experimental setup, MATLAB Simulink software is used. The whole system design is shown in Fig. 10. The variable speed drive for the prime mover started keeping a constant speed from zero to 85-Hz with the V/f-based accelerator mode using sinusoidal PWM, which provides a power of 7.5 kW. The reference speed and frequency together with the output voltage are adjustable in order to keep the air-gap flux linkage constant. The rated power of the mover is 5.5 kW, 400 V, 1440 rpm and 2-pole pairs. The rated power of the SEIG is 3.5 kW, 400 V, 720 rpm and 4-pole pairs.

A three phase exciting capacitor with a fixed value of 2500 VAr is connected to the terminal of the SEIG to obtain a 50-Hz output electrical frequency at full load and to maintain the needed reactive power. The consumer load is totally changed from zero to 2000 W. The modulation index is set to 0.7 and the drive frequency of the mover should be kept at 45-Hz. The internal structures of the Separated Electronic Load Controller, the Fuzzy Logic Controller and the Variable Duty PWM Generator Subsystems are shown in Fig. 3, Fig. 7 and Fig. 11, respectively.

The schedule boxes in the Simulink block diagram, in Fig. 10, are employed to adjust activation time of the converters and the consumer load applications.

To obtain the design parameters of the control system with the generator and to achieve 230 V AC (line to neutral) at the terminal at the rated frequency in the case of driving the mover at 45 Hz, the SEIG is loaded by a total active power of 2000 W according to the total efficiency of the whole system by changing the excitation capacitor. The obtained result is given in Fig. 12(a). From this figure, the reactive power for getting 230-V and 50 Hz at the terminal can be seen. In addition, a capacitor value of 2500-VAr is convenient for this loading condition.

On the other hand, while increasing the total load power at the terminal of the SEIG, the output voltage decreases, as shown in Fig. 12(b). Therefore, the output power of the system at 230 V, the sum of the consumer load and the minimum dumped power are defined at a rated value of 2000-W as the maximum with all of the power loses.

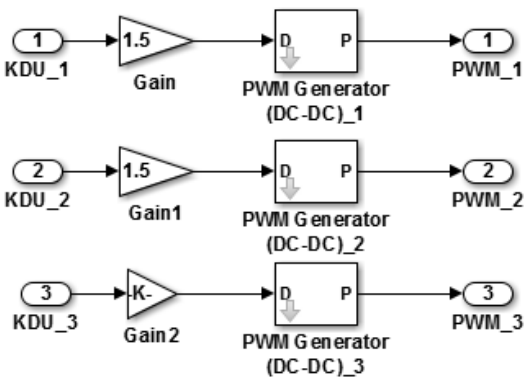

Fig. 11. Internal structure of Variable Duty PWM generator in Simulink block diagram.

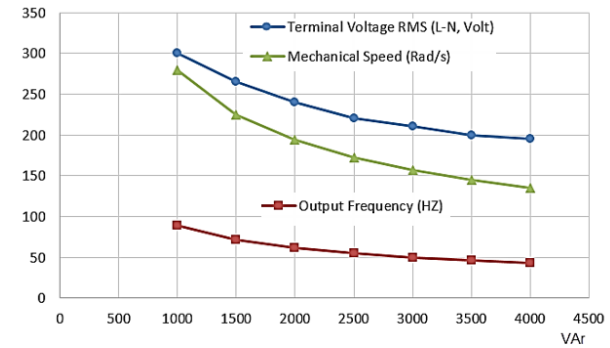

(a)

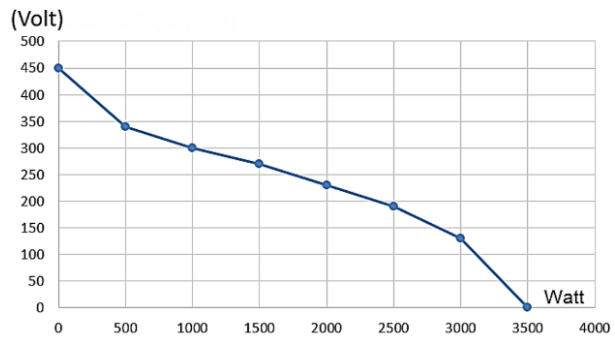

(b)

Fig. 12. (a)Terminal voltage, mechanical shaft speed and output frequency of the SEIG versus excitation capacitor under 2000 W active power, (b) Changing of the terminal voltage (line to neutral) versus total load variation at fixed excitation power of 2500 VAr.(from this figure, total output power of 2000 W is available for getting reference voltage of 230 V).

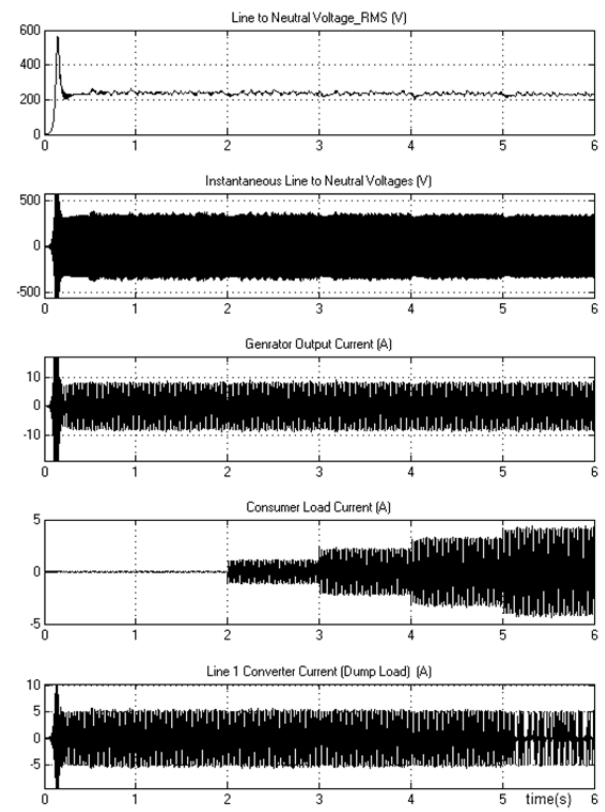

(a)

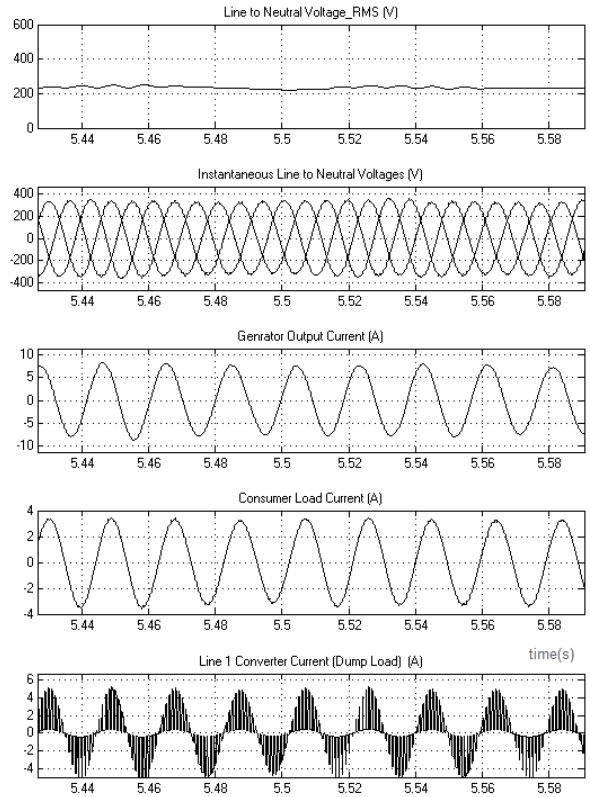

(b)

Fig. 13. Dynamic outputs of the SEIG in transient and steady state, (a) Loading Schedule: *t*=0: No Load, *t*=2s: 500 W, *t*=3s: 1000 W, *t*=4s: 1500 W, *t*=5s: 2000 W, (b) details for 1500 W application.

In simulation studies, both of the converter structures are tested and the obtained results with details under different load conditions are introduced in Fig. 13 to Fig. 15. Fig. 13 shows the transient and steady state behavior of the SEIG versus the consumer load changing from no load to 2000 W.

Fig. 14 shows that the excitation power provided by the fixed capacitor at the terminal is not sufficient in the case of inductive load applications because of the reducing magnetizing current. In addition, a larger capacitor at the terminal under varying loads without exceeding the stator current increases the over load capacity of the generator by resulting in a lower output frequency. On the other hand, the capability of the voltage regulation increases with the ratings of the SEIG. However, resistive load applications do not cause decreases in the frequency.

V. Experimental Setup and Results

In the laboratory, a three-phase induction motor with a variable speed drive is used in place of a wind turbine model. Experimental studies are carried out for different independent consumer loads. Single-phase loads can be used as an unbalanced load through the proposed converter model. SELCs are designed to perform their tasks for the all-loading conditions. In addition, the controller interface includes

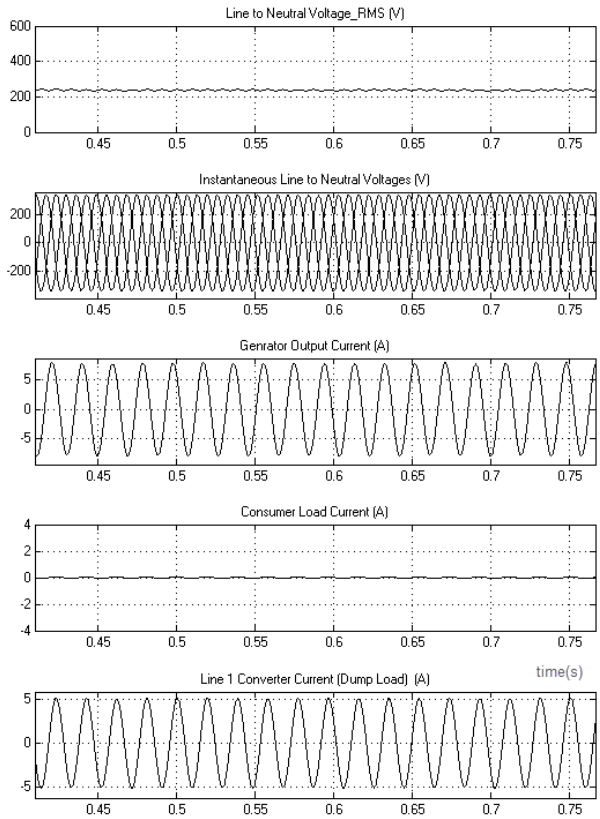

(a)

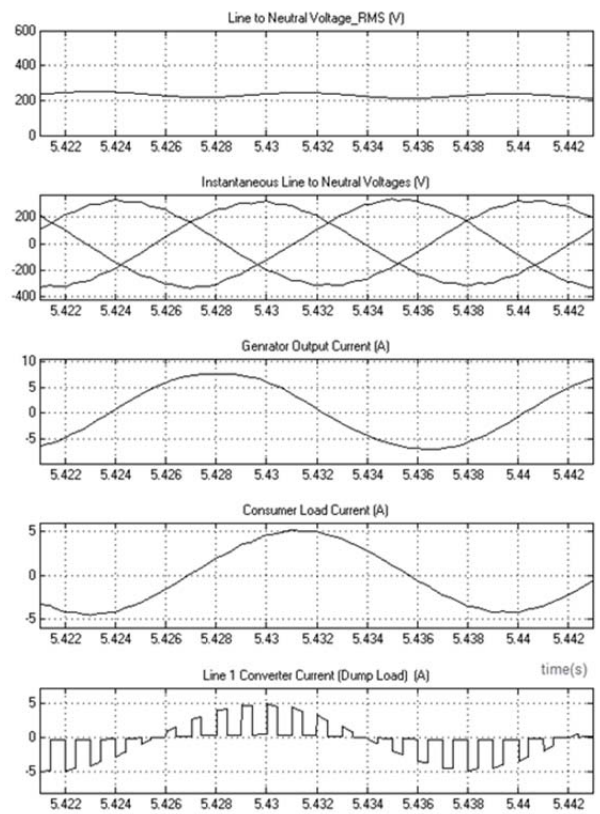

(b)

Fig. 14. (a) No load operation of the SEIG, (b) detail of 2000 W in 0.8 inductive power factor.

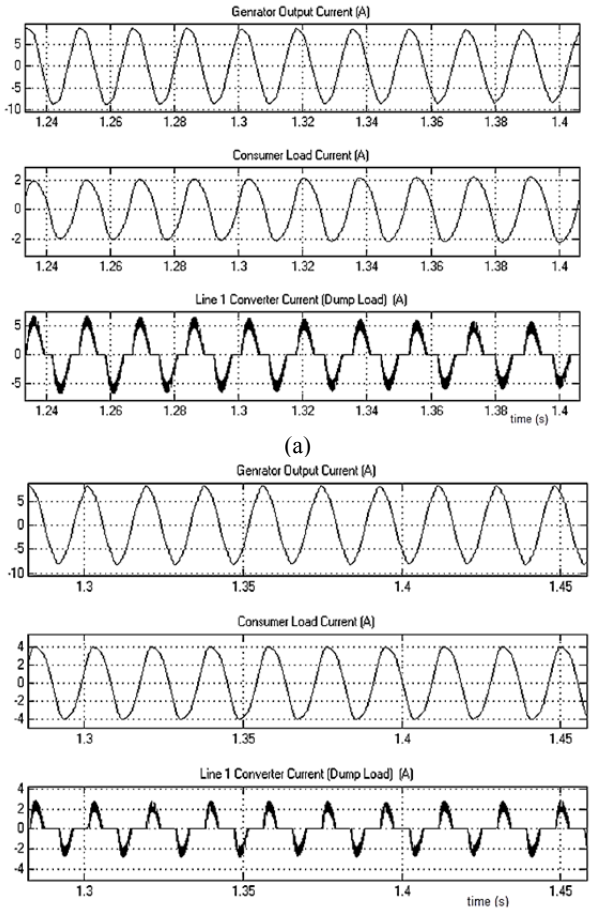

Fig. 15. Details of dynamic outputs of the SEIG by SELC structure with capacitor (R_{d1}=75 Ω, R_{d2}=750 Ω, 230 V, Consumer Load: (a) for 1000 W, (b) for 2000 W.

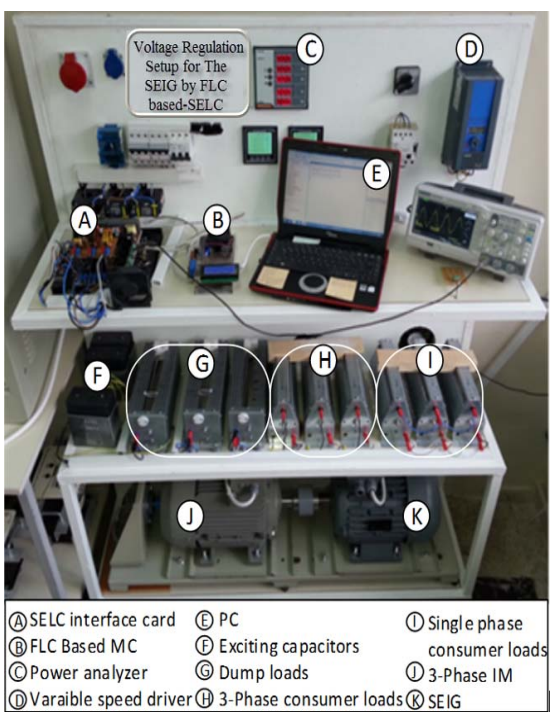

Fig. 16. Experimental setup for the proposed system.

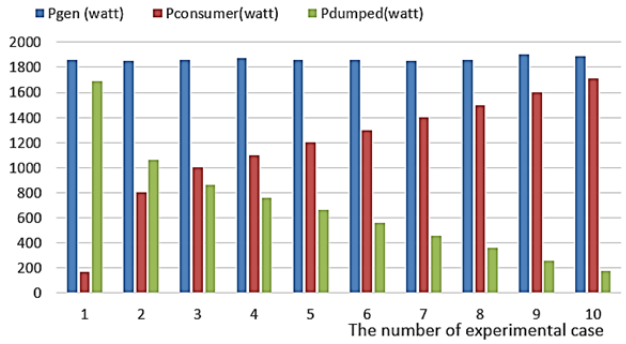

Fig. 17. Experimental results of the generated, consumer and the dumped power variations.

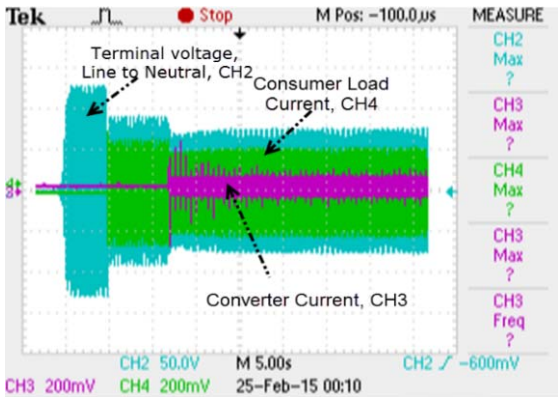

(a)

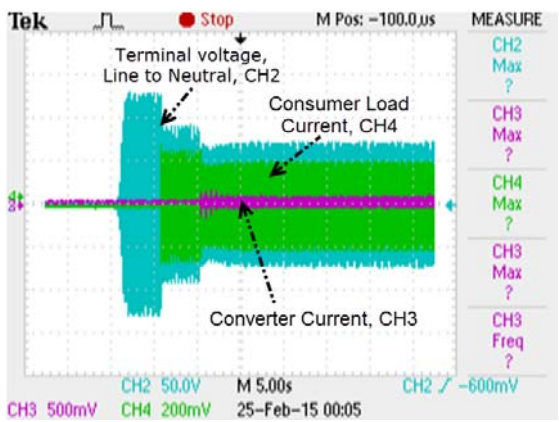

(b)

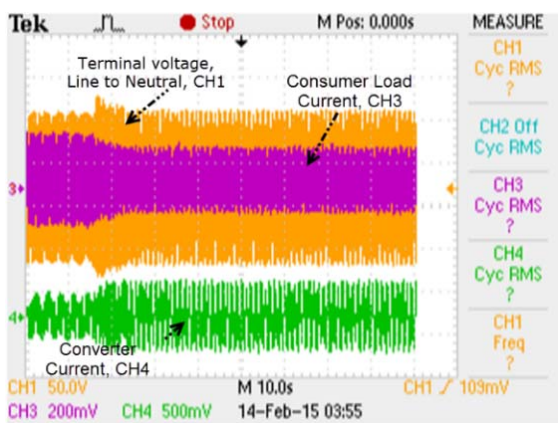

(c)

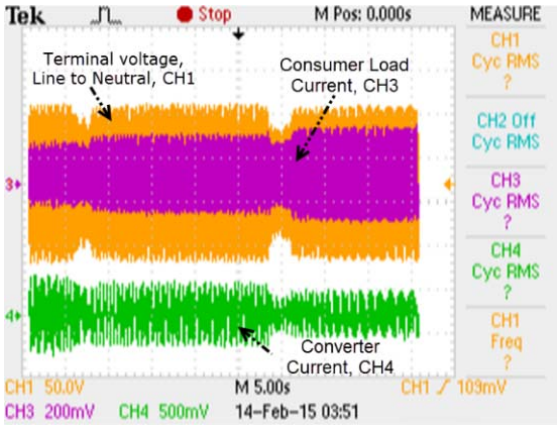

(d)

Fig. 18. Experimental results for the steady state behavior of the SEIG in different loads. Consumer load application (2 A amplitude) after start-up with no load, and controller activation (1 A amplitude) for voltage regulation: (a) application without capacitor mode, (b) application with capacitor mode, (c) decrease in consumer load without capacitor mode, (d) decrease in consumer load with capacitor mode (current sensor scale: 100mv=1A/div, voltage sensor scale: 1x4; 50V=200 V/div).

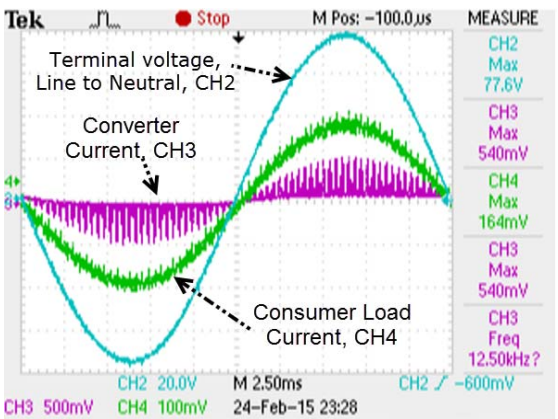

(a)

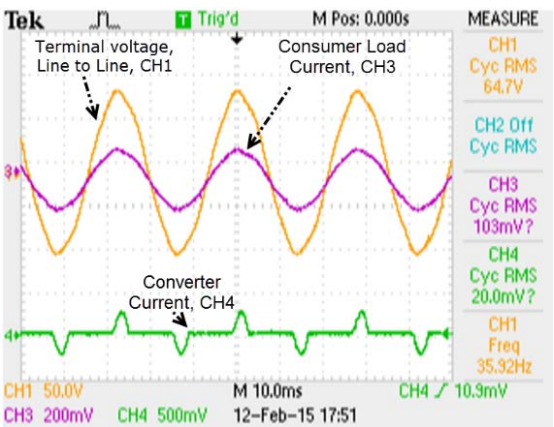

(b)

Fig. 19. Detailed current and voltage waveform in one cycle for both converter structures, (a) without capacitor, (b) with capacitor (Current sensor scale: 100mv=1A/div, Voltage sensor scale: 1x4; 50V=200 V/div, 20V=80V/div).

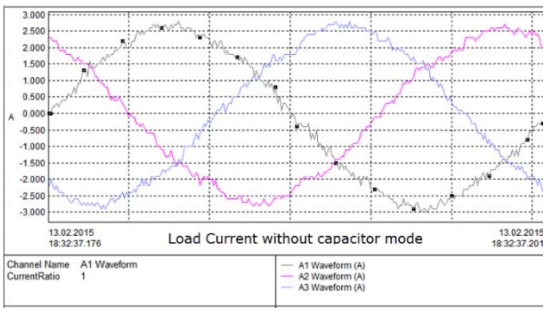

(a)

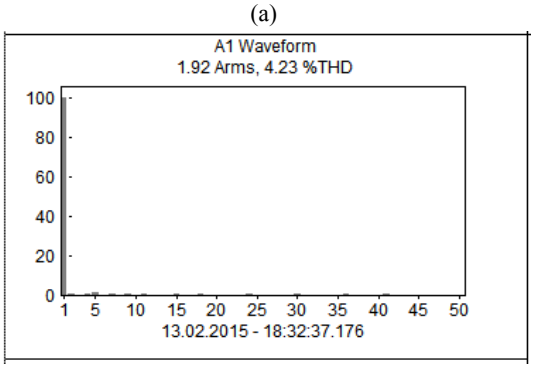

(b)

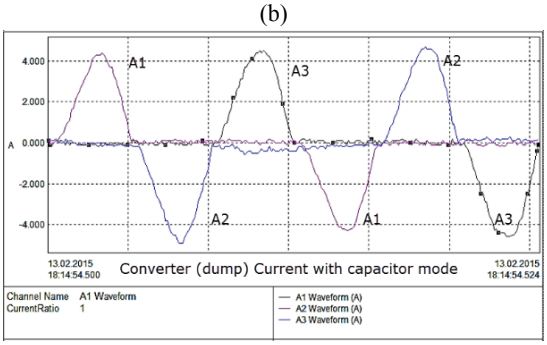

(c)

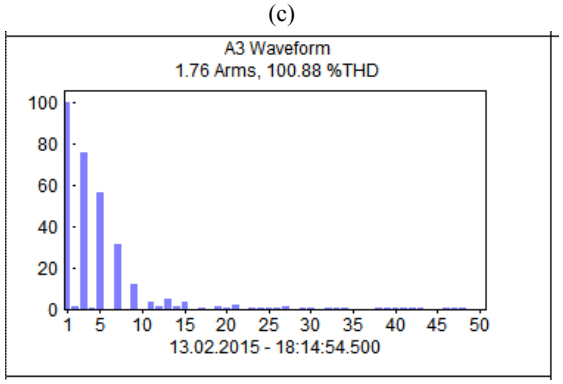

(d)

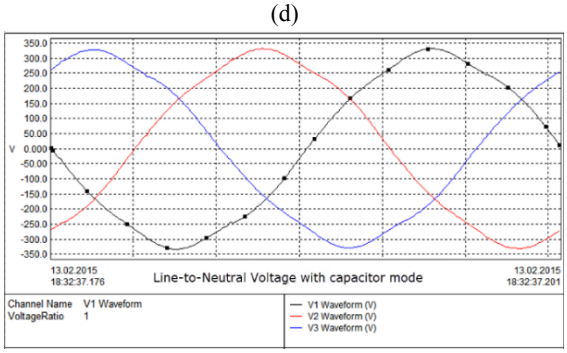

(e)

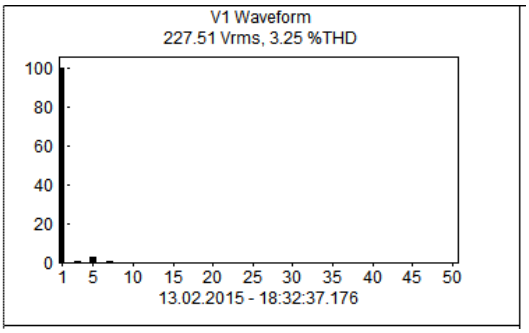

(f)

Fig. 20. Current and voltage waveforms along with the harmonic level and THD of the SEIG and controller for both converter structures, (a) consumer load waveform without capacitor, (b) consumer load THD without capacitor, (c) converter current with capacitor, (d) converter current THD with capacitor, (e) line-to-neutral voltage with capacitor, (f) voltage THD with capacitor.

measurement and monitoring boards. All of the generated, consumed and dumped powers are observed via both a power analyzer and this monitoring display. The full experimental setup is presented in Fig. 16.

For determine the amount of dump load that complements the consumer load variations, ten-different operation cases are carried out on the experimental setup. The obtained results for these cases are illustrated in Fig. 17. All of the produced power except for the loses is transferred to the consumer load if necessary. The opposite is also true. Especially, in the absence of a customer load, when all of the produced power is transferred to the dump loads. On the other hand, in order to keep the terminal voltage and frequency constant, the surplus power is transferred to the dump loads through the SELCs while the consumer load decreases.

Fig. 18 shows the voltage regulation by the SELC after start-up and load applications. Due to used converter structure, current and voltage waveform in both the transient and steady state show differences with respect to each other. When reducing the consumer load, voltage regulation in the capacitor mode, a little perturbation is observed, as shown in Fig. 18(c). In contrast to that, without the capacitor mode, the controller response is very quick with a little exceeding.

The currents drawn by the consumer loads and the SELCs are presented in Fig. 19 for one cycle, and the long-term behaviors of the converters are shown in Fig. 18. The controller in the proposed converter with a capacitor compensates the rectified voltage over the bridge diodes, and the currents are switched between two levels on the hill of the waveform. Thus, because of resistive consuming, while the main current wave resembles a full sine, the controller current wave is rectified and chopped by the IGBT during the duty cycle, as shown in Fig. 19 (b). Therefore, in case of using a higher switching frequency, such as 30-40 kHz, the harmonic order and levels will be reduced in the converter structure without a capacitor.

TABLE II
COMPARISON OF SIMULATION AND EXPERIMENTAL RESULTS

Conv. structure	Cons. Load	Frequency (Hz)		Terminal Voltage Volt		THD %		Current THD % Cons. Load		Dump Load		Generator	
	Watt	Cal.	Exp.	Cal.	Exp.	Cal.	Exp.	Cal.	Exp.	Cal.	Exp.	Cal.	Exp.
Without capacitor	0	50.9	50.0	234	230	4.66	4.23	--	--	4.66	5.02	4.30	4.23
	500	50.2	49.7	231	229	3.17	2.93	3.17	3.03	15.06	17.85	3.43	3.21
	1000	50.0	50.7	232	234	2.53	2.13	2.53	2.25	21.15	20.32	2.58	2.45
	1500	49.8	50.2	231	230	3.92	3.03	3.92	4.02	29.42	27.25	2.05	1.97
	2000 0.8 +	50.8	51.0	227	229	2.45	2.13	2.25	2.40	27.25	26.02	3.44	3.73
With capacitor	0	50.9	50.0	232	230	5.03	4.95	--	--	14.25	15.65	4.52	5.23
	500	49.8	49.5	228	229	4.85	4.23	4.85	4.65	78.52	79.28	4.35	4.75
	1000	49.2	49.0	227	229	4.76	4.35	4.85	4.95	98.58	100.22	5.01	4.95
	1500	49.0	49.0	227	226	4.88	3.25	4.88	4.50	110.1	100.88	6.97	5.63
	2000 0.8+	50.5	50.0	225	227	4.01	4.27	4.05	3.87	100.5	98.95	3.47	4.68

(Conv.: converter, Cal.: calculated, Cons.: consumer, Exp.: experimental, +: inductive power factor)

In Fig. 20, the current and voltage waveforms along with the harmonic order and THD values are illustrated by a power analyzer in the steady state for some instances. It can be seen that the THD value of the main load current is an acceptable limit at less than 5% despite the high harmonic order and level that occures on the converter current. However, in the converter structure with a capacitor the THD value and harmonic order are a lot more than those without the capacitor mode. Therefore, although there is no significant effect on the main currents, eliminating these harmonics is more difficult than the others. On the other hand, the effect of the rectified controller current on the line voltage is considerable from point of of view of the fifth harmonic level. Even if the level is less, the effect must be considered.

VI. CONCLUSION

In this study, two different converter structures are investigated to achieve optimal and low order harmonic voltage regulation for the SEIG. The implementation setups are installed and a lot of experiments are carried out by these converter structures. The obtained results are given and a comparison study is included, as presented in Table II. When evaluating in terms of harmonic and regulation performance, when using a serial pre-dump resistor with a switched dump resistor, the converter structure with no capacitor at the end of the bridge rectifier gives acceptable and good results relative to the with capacitor mode. If the consumer load is resistive, it is very easy to keep the line voltage and frequency constant at desired values. However, in case of an inductive load causing a decrease in the harmonic level, the line voltage decreases and the frequency increases a little bit, due to reductions in the magnetizing current. In particular, the behavior of the proposed converter with a capacitor is newly presented in this paper [Fig. 15 and Fig. 19(b)].

Firstly, via simulations, the design parameters of the experimental setup are determined and the implementation setup is installed with respect to these parameters. The determined capacitor for self-exciting at a fixed value for only dependent balanced loads is enough to maintain a constant frequency at a set value. In addition, for providing needed reactive power under all conditions, the use of switched-capacitor bank is indispensable for achieving a constant voltage and frequency. However, it is shown in this study, as in the literature, the a fixed value for the capacitor is determined at full load operation for a defined frequency under the condition that voltage regulation must be carried out.

It is also concluded that a separated electronic load controller is capable of independend voltage regulation for each phase. In addition, using an IGBT along with an uncontrolled diode rectifier for each phase is cheaper than using a controlled three-phase converter consisting of six-IGBTs and their driver boards, which is only available for three-phase voltage regulation and three-phase balanced consumer loads. In a separate electronic load controller, a small snubber inductance serial connected with the dump load is used to reduce the switching harmonics, which are injected into the consumer load line over the rectifier by the chopper to minimize the switching loses.

From the point of view of harmonic reduction and obtaining high regulation performance, the converter structure with no capacitor at the end of the bridge rectifier gives acceptable and good results with respect to the other structure with a capacitor. The proposed converter models and controllers are available for both low cost applications and independent or unbalanced consumer load operations.

ACKNOWLEDGMENT

This study was supported by Pamukkale University, Scientific Research Projects Coordination Unit (PAU-BAP) under Grant Project Number 2015FBE037.

REFERENCES

[1] K. Natarajan, A. M. Sharaf, S. Sivakumar, and S. Naganathan, "Modeling and control design for wind energy conversion scheme using self-excited induction generators," *IEEE Trans. Power Electron.*, Vol. EC-2, No. 3, pp. 506-512, Sep. 1987.

[2] C. Grantham, D. Sutanto, and B. Mismile, "Steady state and transient analysis of self-excited induction generators," *IEE Proceedings B – Electric Power Applications*, Vol. 136, No. 2, pp. 61-68, Mar. 1989.

[3] B. Singh, "Induction generator-A prospective," *Electric Machines & Power S*ystems, Vol. 23, No. 2, pp. 163-177, 1995.

[4] G. K. Singh, "Self-excited induction generator research-a survey," *Electric Power Systems Research,* Vol. 69, No. 2~3, pp. 107-114, May 2004.

[5] P. C. Krause and C. H. Thomas, "Simulation of symmetrical induction machinery," *IEEE Trans. Power App. Syst.*, Vol. 84, No. 11, pp. 1038–1053, Nov. 1965.

[6] E. D. Bassett and F. M. Potter, "Capacitive excitation for induction generators," *Electrical Engineering,* Vol. 54, No. 5, pp. 540-545, May 1935.

[7] E. Bim, J. Szajner, and Y. Burian, "Voltage compensation of an induction generator with long-shunt connections," *IEEE Trans. Energy Convers*., Vol. 4, No. 3, pp. 526-530, Sep. 1989.

[8] L. Wang and J. Y. Su, "Effects of long-shunt and short-shunt connections on voltage variations of a self-excited induction generator," *IEEE Trans. Energy Convers.,* Vol. 12, No. 4, pp. 368-374, Dec. 1997.

[9] L. Shridlar, B. Singh, C. S. Jha, B. P. Singh, and S. S. Murthy, "Selection of capacitors for the self-regulated short shunt self-excited generator," *IEEE Trans. Energy Convers.,* Vol. 10, No. 1, pp. 10-17, Mar. 1995.

[10] S. N. Mahato, S. P. Singh, and M. P. Sharma, "Capacitors required for maximum power of self-excited single-phase induction generator using a three-phase machine," *IEEE Trans. Energy Convers.*, Vol. 23, No. 2, pp. 372-381, Jun. 2008.

[11] R. Pena, J. C. Clare, and G. M. Asher, "A doubly fed induction generator using back-to-back PWM converters supplying an isolated load from a variable speed wind turbine," *IEE Proceedings - Electric Power Applications*, Vol. 143, No. 5, pp. 380-387, Sep. 1996.

[12] B. Shing and G. K. Kasal, "Solid state voltage and frequency controller for a stand-alone wind power generating system," *IEEE Trans. Power Electron.*, Vol. 23, No. 3, pp. 1170-1177, May 2008.

[13] F. Giraud and Z. M. Salameh, "Wind-driven variable-speed, variable frequency, double-output, induction generators," *Electric Machines & Power Systems*, Vol. 26, No. 3, pp. 287-297, 1998.

[14] U. K. Madawala, T. Geyer, J. B. Bradshaw, and D. M. Vilathgamuwa, "Modeling and analysis of a novel variable-speed cage ınduction generator," *IEEE Trans. Ind. Electron.,* Vol. 59, No. 2, pp. 1020-1028, Feb. 2012.

[15] A. F. Attia, H. Soliman, and M. Sabry, "Genetic algorithm based control system design of a self-excited induction generator," *Acta Polytechnica – Journal of Advanced Engineering,* Vol. 46, No. 2, pp.11-22, 2006.

[16] H. F. Soliman, A. F. Attia, S. M. Mokhymar, and M. A. L. Badr, "Fuzzy algorithm for supervisory voltage/frequency control of a self-excited induction generator," *Acta Polytechnica – Journal of Advanced Engineering,* Vol. 46, No. 6, pp. 36-48, 2006.

[17] H. Geng, D. Xu, B. Wu, and W. Huang, "Direct voltage control for a stand-alone wind-driven self-excited ınduction generator with ımproved power quality," *IEEE Trans. Power Electron.*, Vol. 26, No. 8, pp. 2358-2368, Aug. 2011.

[18] G. K. Kasal and B. Singh, "DSP-based voltage controller for an isolated asynchronous generator feeding induction motor loads," *Electric Power Components and Systems,* Vol. 37, No. 8, pp. 914-935, Jun. 2009.

[19] T. Yamamoto, F. Yamamitsu, and T. Sonoda, "Voltage control of self-excited induction generators using a three-phase magnetic flux controlled type variable reactor," *Journal of International Council on Electrical Engineering,* Vol. 2, No. 3, pp. 309-316, Jun. 2012.

[20] R. Bonert and G. Hoops, "Stand-alone induction generator with terminal impedance controller and no turbine controls," *IEEE Trans. Energy Convers.,* Vol. 5, No. 1, pp. 28-31, Mar. 1990.

[21] R. Bonert and S. Rajakaruna, "Self-excited induction generator with excellent voltage and frequency control," *IEE Proceedings - Generation, Transmission and Distribution,* Vol. 145, No. 1, pp. 33-39, Jan. 1998.

[22] B. Singh, S. S. Murty, and S. Gupta, "Transient analysis of self-excited induction generators with electronic load controller supplying static and dynamic loads," *IEEE Trans. Ind. Appl.,* Vol. 41, No. 5, pp. 1194-1204, Sep./Oct. 2005.

[23] B. Singh, S. S. Murty, and S. Gupta, "Analysis and design of electronic load controller for self - excited induction generators," *IEEE Trans. Energy Convers.,* Vol. 21, No.1, pp. 285-293, Mar. 2006.

[24] B. Singh, S. S. Murty, and S. Gupta, "A voltage and frequency controller for self-excited induction generators," *Electric Power Components and Systems*, Vol. 34, No. 2, pp. 141-157, 2006.

[25] S. A. Deraz and F. E. Abdel Kader, "A new control strategy for a stand-alone self-excited induction generator driven by a variable speed wind turbine," *Renewable Energy*, Vol. 51, pp. 263-273, Mar. 2013.

[26] J. M. Ramirez and M. E. Tores, "An electronic load controller for the self-excited ınduction generator," in *IEEE Power Engineering Society General Meeting*, pp.1-8, Jun. 2007.

[27] D. K. Palwalia and S. P. Singh, "New load controller for Single-phase self-excited induction generator," *Electric Power Components and Systems*, Vol. 37, No. 6, pp. 658-671, May 2009.

[28] D. K. Palwalia and S. P. Singh, "Digital signal processor based fuzzy voltage and frequency regulator for self-excited induction generator," *Electric Power Components and Systems,* Vol. 38, No. 3, pp. 309-324, Jan. 2010.

[29] M. Tariq and S. Yuvarajan,"Modeling and analysis of self-excited induction generator with electronic load controller supplying static loads," *Canadian Journal on Electrical and Electronics Engineering*, Vol. 4, No. 1, pp. 9-12, Feb. 2013.

[30] S. S. Gao, G. Bhuvaneswari, S. S. Murthy, and U. Kalla, "Efficient voltage regulation scheme for three-phase self-excited induction generator feeding single-phase load in remote locations," *IET Renewable Power Generation,* Vol. 8, No. 2, pp. 100-108, Mar. 2014.

[31] S. Archana and A. R. Kumar, "Three phase self-excited induction generator electronic load controller using PI

controller," *International Journal of Advanced Research in IT and Engineering*, Vol. 3, No.5, pp. 21-24, 2014.

[32] P. K. Singh and Y. K. Chauhan, "Performance analysis of multi-pulse electronic load controllers for self-excited induction generator," in *International Conference on Energy Efficient Technologies for Sustainability* (ICEETS), pp. 1299-1307, Apr. 2013.

[33] E. Najafi, A. H. M. Yatim, and A. S. Samosir, "Design and implementation of a dynamic evolution controller for single-phase inverters with large load changes," *Electric Power Components and Systems*, Vol. 42, No. 10, pp. 995-1003, Jun. 2014.

[34] S. Kumari and G. Bhuvaneswari, "Voltage regulation of a stand-alone three-phase SEIG feeding single-phase loads," in *IEEE Students' Conference on Electrical, Electronics and Computer Science (SCEECS)*, pp. 1-6, Mar. 2014.

[35] R. Pena, R. Cardenas, E. Escobar, J. Clare, and P. Wheeler, "Control system for unbalanced operation of stand-alone doubly fed ınduction generators," *IEEE Trans. Energy Convers.*, Vol. 22, No. 2, pp. 544-545, Jun. 2007.

[36] L. A. Zadeh, "Fuzzy sets," *Information and Control*, Vol. 8, No. 3, pp. 338-353, Jun. 1965.

[37] A. Abraham, *Rule-based expert systems*, Handbook of Measuring System Design, Edited by Sydenham, P. and Thorn, R., Vol. 2, John Willey & Sons, New York, 2005.

[38] S. Kesler, A. S. Akpınar, A. Saygın, and Y. Oner, "DSP implementation of a variable speed drive using fuzzy logic based voltage injection method for wound-rotor induction machines," *International Review of Electrical Engineering (IREE)*, Vol. 3, No. 6, pp. 962-974, Nov./Dec. 2008.

[39] T. Takagi and M. Sugeno, "Fuzzy identification of systems and its applications to modeling and control," *IEEE Trans. Syst., Man, Cybern.*, Vol. SMC-15, No. 1, pp. 116-132, Jan./Feb. 1985.

[40] E. H. Mamdani and S. Assilian, "An experiment in linguistic synthesis with a fuzzy logic controller," *International Journal of Man-Machines Studies*, Vol. 7, No. 1, pp. 1-13, Jan. 1975.

Selami Kesler received his B.S., M.S., and Ph.D. degrees from the Karadeniz Technical University, Trabzon, Turkey, in 1991, 1998, and 2006, respectively, all in Electrical Engineering. He joined the Karadeniz Technical University in 1992, where he worked as a Lecturer until 2004. He joined the Department of Electrical Education, Pamukkale University, Denizli, Turkey, in 2004, as a Lecturer, where he has been an Associate Professor in the Department of Electrical Engineering, since 2011. His current research interest include power electronics, AC drives, the dynamic analysis of electrical machines, intelligent control techniques, advanced DSP technologies and power conversion systems.

Tayyip L. Doser received his B.S. and M.S. degrees from Pamukkale University, Denizli, Turkey, in 2007 and 2014, respectively. From 2010 to 2015, he worked as an Operations Manager of a cogeneration power plant at a textile firm in Denizli, Turkey. Since 2015, he has been working as an Operations Manager at a hydropower plant in the Denizli region, Turkey. His current research interests include power electronics, renewable energy and the efficiency of generators.